Buckling Response and Elastic Stiffness of Butterfly Dampers

Behrokh Hosseini Hashemi[1]* and Babak Keykhosro Kiani[2]

1. Associate Professor, Structural Engineering Research Center, International Institute of Earthquake Engineering and Seismology (IIEES), Tehran, Iran,
*Corresponding Author; email: behrokh@iiees.ac.ir
2. Ph.D. Candidate, Structural Engineering Research Center, International Institute of Earthquake Engineering and Seismology (IIEES), Tehran, Iran

ABSTRACT

Butterfly dampers dissipate energy through the flexural, shear, or axial response of the strips when the device is subjected to inelastic cyclic deformation. The buckling response, elastic stiffness, and cyclic performance of non-uniform steel butterfly dampers have been studied in this paper. Validated material and geometric nonlinear finite element models in the ABAQUS has been used to perform a comprehensive parametric study on a wide range of geometrical parameters to evaluate the response of non-compact butterfly dampers. The results showed that although the low-cycle-fatigue response of butterfly dampers can be improved by altering the side edge shapes, the buckling capacity and elastic stiffness of non-uniform strips would decrease in comparison with uniform ones. Hence several analytical equations were provided to quantitative prediction of the buckling capacity and elastic stiffness of butterfly dampers

1. Introduction

The utilization of energy dissipative devices represents a common strategy to protect structures against seismic excitations. Energy dissipating devices are not typically installed in the gravity load path of the structures and are accessible after the earthquake to be inspected for the possible local damages. Replaceability of these devices would significantly decrease the repairing cost of the whole structures after the earthquake.

Among the most used hysteretic damper types, butterfly dampers (BD) have been widely investigated as an effective protection technology able to provide large energy dissipation capacity, with the possibility of easily controlling of both stiffness and strength [1-2]. BDs generally consist of a set of parallel metallic strips connected through a couple of support plates (see Figure 1) and dissipate energy through the flexural and axial mechanisms, when subjected to in-plane deformation demands.

Ghabraie et al. [3] applied an optimization method to optimize the shape of butterfly dampers to improve the stress distribution. Maximizing the hysteretic energy dissipated by the damper after one cycle of displacement loading with a 10% drift amplitude was the objective function. The experimental verification showed that by changing the shape of strips from uniform to an hourglass-shaped, the low-cycle-fatigue response of samples, significantly improved. Xian et al. [4] showed that the non-uniform BDs are expected to initiate yielding at the quarter points, midway between the wider ends and reduced middle section and are capable of full hysteretic behavior up to 0.3 rad shear angle over the link length with the expense of lower initial stiffness and a pinched cyclic response. Lee et al. [2] proposed non-uniform steel strip dampers to improve the fatigue response.
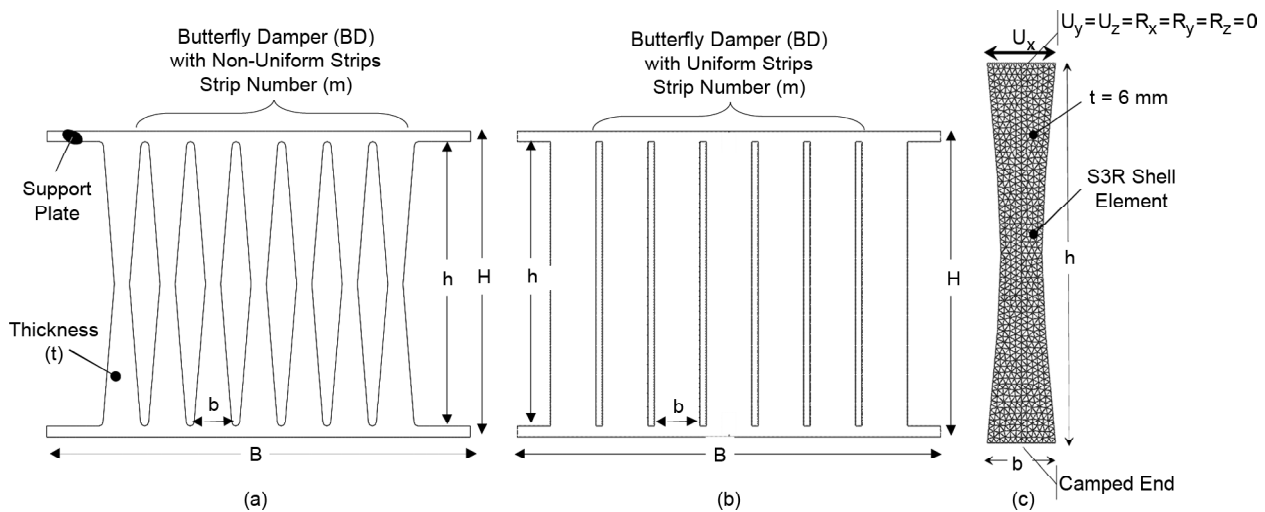
Figure 1. Butterfly damper: (a) with non-uniform strip shape (b): with uniform strip shape. (c): Finite element model of a single strip butterfly damper.

The proposed dampers showed excellent cyclic performance. The structural characteristics such as elastic stiffness, cumulative ductility, and energy absorption were evaluated. According to the test results, the alteration of the side edges and mid-width in strips, affects the ultimate capacity, ductility, and stiffness of the strips [5].

The effect of altering the geometry of steel strips on the low-cycle-fatigue resistance and ductility of yielding dampers has been a subject of interest of many other researchers during the past decade [3, 6,7]. Although the results suggest that it may be possible to provide more uniform plastic strain distribution along the yielding devices such as BDs by changing the edge shapes, removing materials from the original uniform strips could have a negative effect on the buckling response and elastic stiffness of strips. Furthermore, a pinched hysterics response can be anticipated in the case of non-compact, non-uniform BDs.

In this study, a set of empirical equations are proposed to predict the initial elastic stiffness and buckling capacity of butterfly dampers. For this aim, first, a detailed finite element model was created to accurately capture the cyclic response of a butterfly damper sample against past experimental studies [4] to evaluate the effect of non-uniform edge shapes on the response of BDs. Following that, a sensitivity study is performed to ensure that the results are not mesh-dependant. More than 10,000 FE models with random non-uniform shapes and 180 single strip FE models with uniform shapes were also analysed to

study the buckling response and elastic response of non-uniform single strips. The cyclic response of uniform and non-uniform single strip models was also evaluated in terms of pinching response.

2. Finite Element Modeling

The nonlinear analyses in this study have been carried out in ABAQUS/Standard. The FE model details such as mesh density, element type, and boundary conditions are shown in Figure (2). The experiment results carried out by Xian et al. [4] on a butterfly damper (B09-56 sample), have been used in order to verify the finite element models. The geometrical dimensions (in mm) for the B09-56 sample as well as the test setup are shown in Figures (2a) and (2b). The material characteristics based on measured results from coupons test (Plate C), provided in [4], was used in the FEM analysis. The engineering yield stress and ultimate stress of material were about 347 and 435 Mpa respectively and the ultimate strain was about 18%. The AISC341-05 [8] loading history for link-to-column connections in eccentrically braced frames with minor modifications was adopted in the test. A mesh refinement analysis was also conducted to ensure that the results converged on an accurate solution. The B09-56 model was analyzed with different mesh sizes ranging from b/5 to b/40. Figure (2e) shows the incremental change in the maximum value of equivalent plastic strain (PEEQ) observed along the B09-56 model when the initial cracks appeared in the corresponding test sample, as
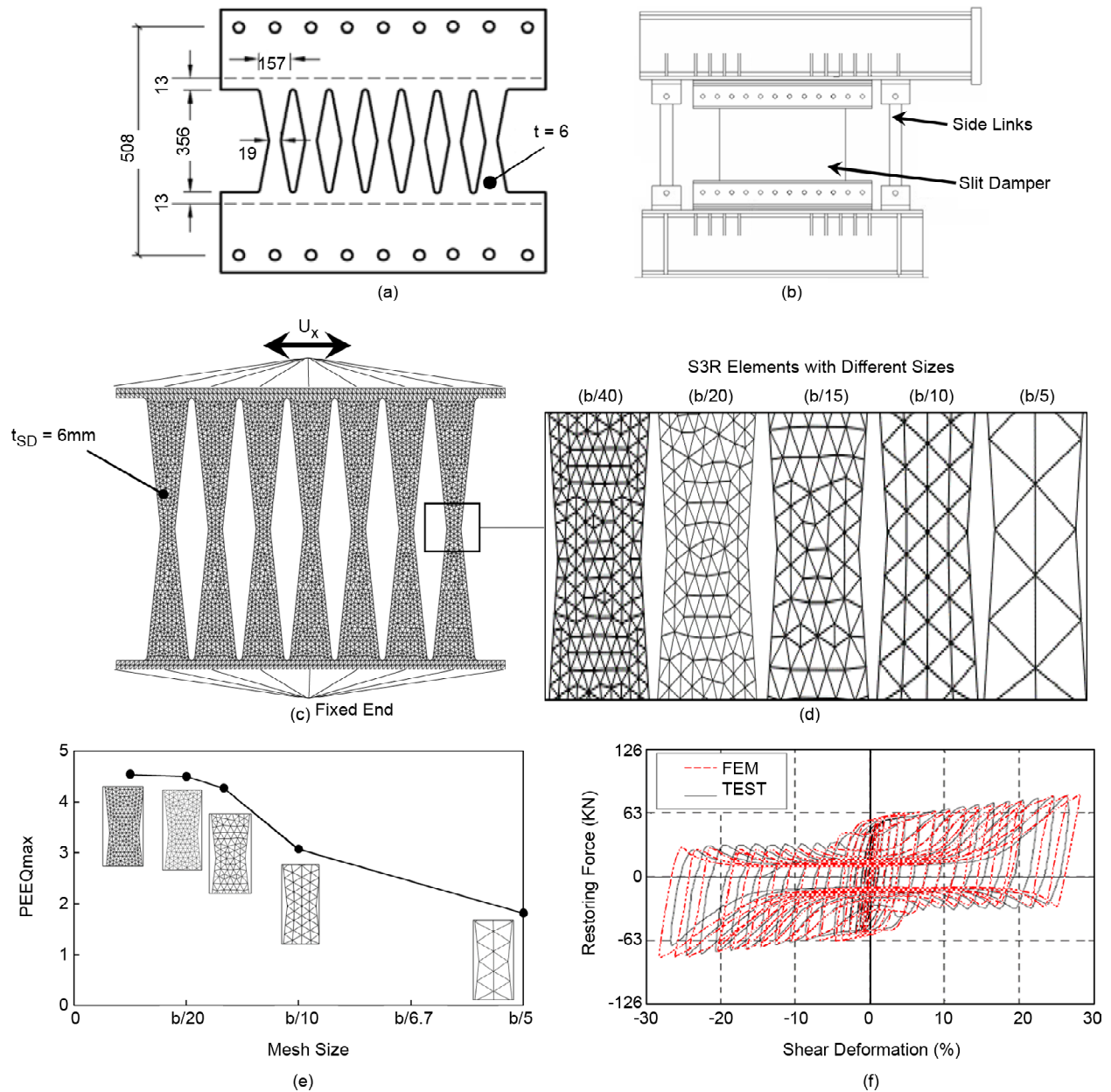
Figure 2. Comparison between experiment and FEM results: (a) The geometrical dimensions (in mm) of B09-56 specimen. (b): The test setup configuration. (c): Finite element details of the B09-56 model. (d): different mesh densities that were considered in the mesh density analysis. (e): Element size versus incremental change in PEEQmax. (f): Comparison of cyclic response of B09-56 specimen and FE model created in this study.

was reported in [4]. As shown, by taking a mesh size equal or smaller than b/20, no significant variation observed in the plastic response of model.

The finite element model was composed of S3R shell elements, with a maximum element size of 3 mm (about b/20). Initial geometric imperfections were explicitly incorporated in the SSBD numerical models to mobilize the buckling response of the yielding plates [8]. A global geometrical imperfection associated with the first local buckling eigen-mode with an amplitude equal to one percent of the sample height (3.5 mm) was included in the finite element

model. More details of the experiment are presented in [4]. The cyclic response of the sample observed in the experimental test and FE models at the end of prescribed loading are compared in Figure (2f). Comparisons of the responses of the analytical models and the experimental results have shown that the utilized finite element model successfully captured the load-deformation response of the butterfly damper.

Xian et al. [4] showed that the number of strips in BDs does not have a major impact on the normalized behavior of BDs. Hence, in order to reduce the

computational costs, the finite element process in the parametric study in this paper is carried out on the single strip butterfly damper (SSBD) models as is depicted in Figure (3a). Other FE details, including material properties, boundary conditions, and initial geometric imperfection were similar to the FE model which was generated in the validation study (Figure 2c).

3. Geometrical Parameters of the Butterfly Dampers

In this study, two groups of FE models were generated. The first group of FE models consisted of 24 basic Single Strip Butterfly Damper (SSBD) models with four different heights (h) and six aspect ratios (h/b) and constant plate thickness equal to 6 mm as are presented in Table (1). More than 10,000 random models created based on basic models with a few geometrical restrictions to avoid the generation of unreasonable non-uniform shapes during the finite element updating process according to non-uniform shapes suggested in [7, 9, 10].

Each strip is assumed doubly symmetric with respect to the center of the plate and an upper bound for the coordination of control points (X^i based on Figure (3a)), equals to 0.45 percent of strip width

(0.45b) is also considered. In order to prevent jagged boundary lines in the resulted shapes, the ($x^{i+1} \geq x^i$) is also added to the finite element updating restrictions. A schematic figure from non-uniform strips and the imposed restrictions are depicted in Figure (3a). The FEMA-461 [11] loading history (See Figure 3b) employed to evaluate the accumulated damage due to cyclic loading with incremental amplitudes. According to Figure (3b), Δ_o is the lowest damage state amplitude and conservatively considered equal to 0.1 % in this study, which is much less than the yield or buckling deformation of SSBD models. Each increment consists of two cycles and after each iteration of loading, the displacement amplitude was increased by a factor of 1.4.

According to the previous studies [7, 12, 13, 14], although BDs are capable of providing substantial ductility and energy dissipation, they are prone to buckling as a major limit state. In order to determine
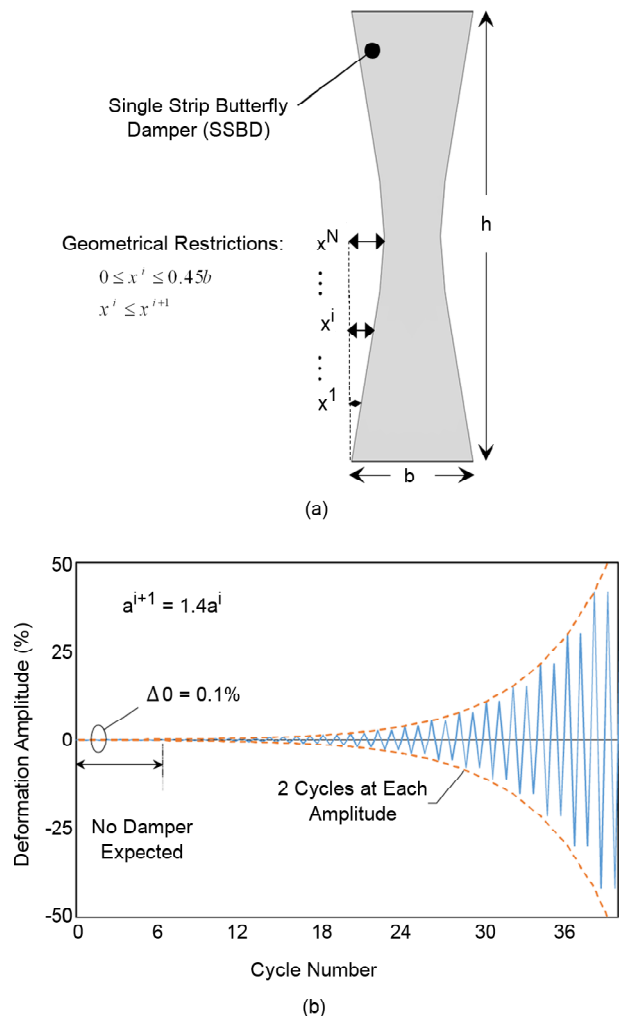
Table 1. Geometrical parameters of basic models with non-uniform shape (group 1).

Group Name	h (mm)	t (mm)	b (mm)	h/b	b/t	h/t
SL90	90	6	7.5	12	1.25	15
			9	10	1.5	
			11.25	8	1.875	
			15	6	2.5	
			22.5	4	3.75	
			45	2	7.5	
SL180	180	6	15	12	2.5	30
			18	10	3	
			22.5	8	3.75	
			30	6	5	
			45	4	7.5	
			90	2	15	
SL360	360	6	30	12	5	60
			36	10	6	
			45	8	7.5	
			60	6	10	
			90	4	15	
			180	2	30	
SL540	540	6	45	12	7.5	90
			54	10	9	
			67.5	8	11.25	
			90	6	15	
			135	4	22.5	
			270	2	45	

Geometrical Restrictions:
$$0 \leq x^i \leq 0.45b$$
$$x^i \leq x^{i+1}$$

(a)

$a^{i+1} = 1.4a^i$

$\Delta 0 = 0.1\%$

No Damper Expected

2 Cycles at Each Amplitude

(b)

Figure 3. (a): Restrictions applied to the geometry of non-uniform single strips (b): Loading history for finite element updating analysis (FEMA- 461).

the elastic buckling response of SSBD models with uniform edges, in the second group of FE models, 180 supplementary FE models with uniform edges were also created due to the lack of enough uniform SSBD models during finite element updating process carried out on the FE models in the first group. The height of complementary models was between 100 to 500 mm with the 100 mm intervals. Other geometrical properties of complementary FE models such as (h/t), (b/t), (h/b) are summarized in Table (2). The results obtained from the random non-uniform (group 1) and uniform (group 2) models were used to study the effect of non-uniform edge shapes on the response of BDs.

Hedayat [15], proposed a set of tri-linear compactness limits based on a comprehensive FE study, for maximum allowable overall slenderness (h/t) and overall aspect ratio (h/b) in term of cross-sectional

Table 2. Geometrical parameters of supplementary SSBD FE models with uniform edges (group 2).

h (mm)	h / t	h / b
[500,400,300,200,100]	[120, 100, 80, 60, 40, 20]	[12, 10, 8, 6, 4, 2]

aspect ratio (b/t) to avoid buckling in BDs as shown in Figure (4a). The compactness of FE models in groups 1 and 2 are presented in Figures (4a) and (4b) respectively. According to Figure (4), except for FE models with 90 mm in height (SL 90 group) in the first group, the others are non-compact.

4. Results

4.1. The Buckling Response of BDs

The critical shear buckling stress (τ_{cr}) of a plate, subjected to edge shear can be expressed by Equation (1).

$$\tau_{cr} = \frac{k_s \pi^2 E}{12 (h/t)^2 (1 - v^2)} \tag{1}$$

where k_s is the buckling coefficient, depending on the plate geometry and edge conditions, E is the elastic modulus of material, v is the Poisson's ratio, h is the plate height and finally, t is plate thickness (see Figure 1). Although several studies [16-17] has been carried out on buckling response of shear panels (with an aspect ratio, (h/b)<1), relatively little research has been carried out to assess buckling
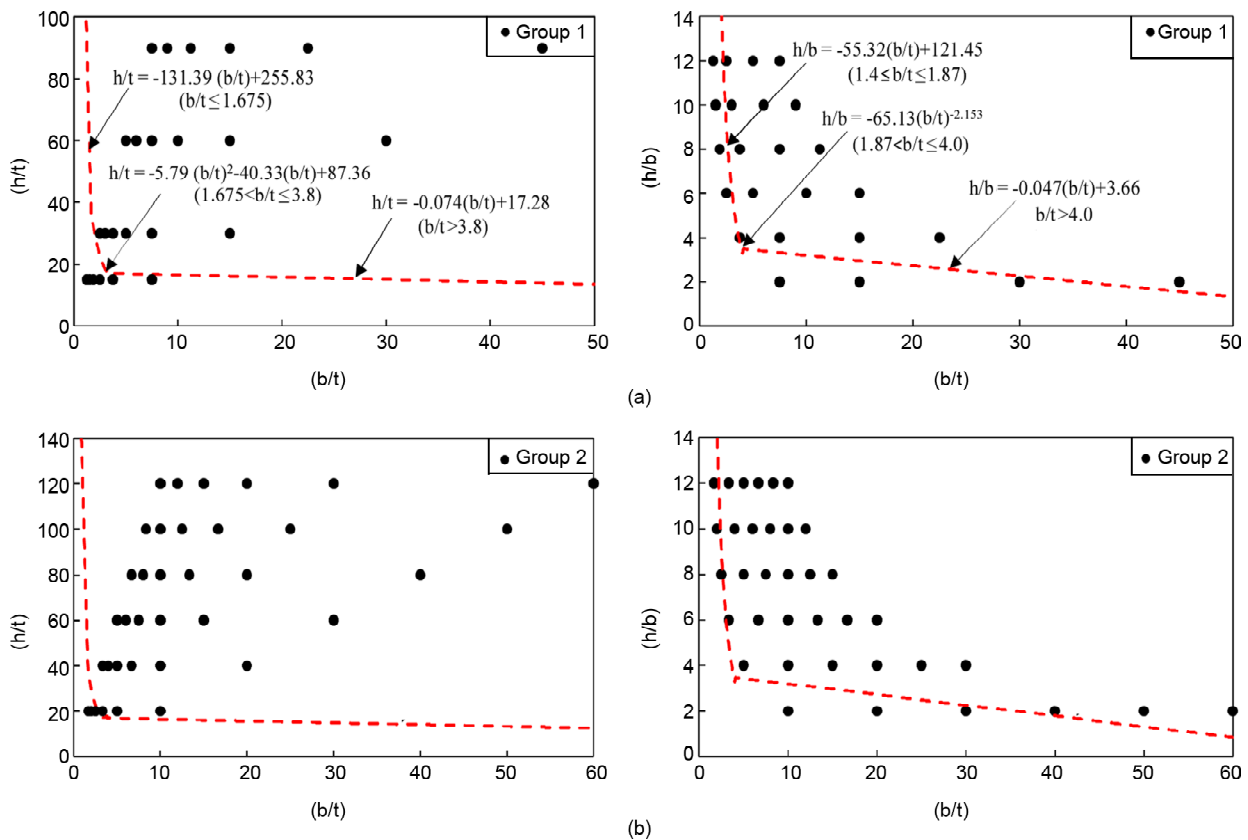

Figure 4. Slenderness status of samples base on the slenderness relationship proposed in [15]. (a): FE models in group 1. (b): FE models in group 2.

behavior of butterfly dampers and even less on the buckling response of BDs with non-uniform edges. The Effect of axial demand due to gravitational loads on the buckling response of strips was not considered in this study.

The buckling coefficient of uniform strips, $k_{S,SSBD}^{uniform}$, obtained from FE models for uniform SSBD models (group 2 of FE models) are presented in Figure (5). As shown, the $k_{S,SSBD}^{uniform}$ values are inversely correlated with (t/b) and (b/h) parameters. According to the results, a regression analysis has been conducted to propose an empirical equation for reliable estimation of $k_{S,SSBD}^{uniform}$. The observed correlation between $k_{S,SSBD}^{uniform}$ and key parameters can be explained by Equation (2). The C_1 and C_2 variables in Equation (2) can be expressed with second-order polynomial relationships, which take into account the influence of (t/b) and overall aspect ratio (b/h) respectively. The minimum R-squared (R^2) value and average error between FEM results and the values obtained from Equation (2) were 0.9996 and 0.4% respectively.

$$k_{S,SSBD}^{uniform} = C_1 C_2 + C_3$$
$$R^2 = 0.9996 \tag{2}$$

$$C_1 = 10^{-5}\left(596.894\left(\frac{t}{b}\right)^2 - 3.274\left(\frac{t}{b}\right) + 19.820\right) \tag{3}$$

$$\frac{t}{h} \le 0.025 \quad C_2 = \left(10843.838\left(\frac{b}{h}\right)^2 + 9763.908\left(\frac{b}{h}\right) - 387.535\right) \tag{4}$$

$$C_3 = 3.194 \tag{5}$$

$$C_1 = 10^{-5}\left(1.786\left(\frac{t}{b}\right)^2 - 30.344\left(\frac{t}{b}\right) + 7.919\right) \tag{6}$$

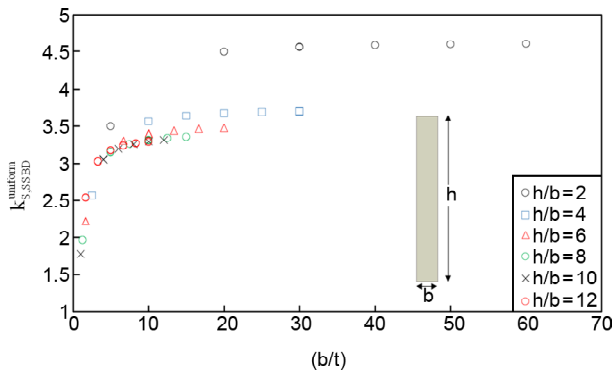$$\frac{t}{h} > 0.025 \quad C_2 = \left(16725.802\left(\frac{b}{h}\right)^2 + 34499.898\left(\frac{b}{h}\right) - 2537.931\right) \tag{7}$$

$$C_3 = 3.050 \tag{8}$$

In Figure (6), the ratio of buckling coefficient obtained of SSBDs with random, non-uniform edges, $k_{S,SSBD}^{non-uniform}$, and the $k_{S,SSBD}^{uniform}$ obtained for uniform SSBDs (Equation 2) are plotted versus the $X_{N.A}$ which can be defined as the normalized average coordination of control points with respect to strip width ($X_{N.A} = \sum X^i / N.b$ according to Figure 3a). The $X_{N.A}$ can also be presented as the ratio of the area of removed parts to the area of corresponding uniform strips.

As shown in Figure (6), the $k_{S,SSBD}^{non-uniform} / k_{S,SSBD}^{uniform}$ ratio exhibited a strong linear correlation with $X_{N.A}$ which can be expressed as follows:

$$k_{S,SSBD}^{non-uniform} = k_{S,SSBD}^{uniform} \times$$
$$(-2.308X_{N.A} + 1.0503) \le k_{S,SSBD}^{uniform} \quad X_{N.A} \le 0.4 \tag{9}$$

The average difference between Equation (9) and the FE results was about 4%. The existing error is largely due to the fact that although variable $X_{N.A}$ seems to be an appropriate, easy to compute variable; however, the $X_{N.A}$ does not necessarily represent the shape of the strips. In other words, different curves can be assumed with different buckling behavior but with the same $X_{N.A}$. Finally, according to Equations (2) and (9), for a conventional BD with arbitrary strip shapes (see Figure 1a), the buckling strength (P_{cr}) can be expressed by the Equation (10).

Figure 5. The buckling coefficient of single strip SSBDs with uniform side edges.
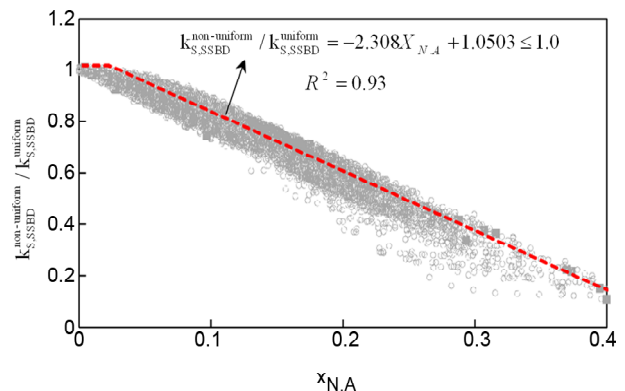

Figure 6. The $k_{S,SSBD}^{non-uniform}$ value for non-uniform single strip SSBD.

The geometrical variables are defined in Figure (1).

$$P_{cr} = mbt \frac{k_{S,SSBD}^{non-uniform} \pi^2 E}{12(h/t)^2(1-v^2)} \quad (10)$$

4.2. Elastic Stiffness of BDs

Similar to the procedure previously used to study the buckling response of BDs with arbitrary non-uniform edge shapes, the elastic stiffness of uniform SSBDs was first studied using the results obtained from uniform FE models, and then the elastic stiffness of uniform models was generalized to BDs with non-uniform side edges based on the results obtained from random non-uniform FE models.

To establish an analytical expression for elastic stiffness of SSBDs with uniform edges ($k_{0,SSBD}^{uniform}$), the stiffness can be described in the form of Equation (11) where $k_{0,N}^{uniform}$ is normalized stiffness of uniform SSBD and can be expressed by a quartic polynomial expression, achieved by regression analysis. The R-squared and average errors are 0.993 and 1% respectively. The $k_{0,N}^{uniform}$ trend with respect to the (h/b), obtained from uniform SSBD, FE models is presented in Figure (7a).

$$k_{0,SSDS}^{uniform} = k_{0,N}^{uniform} Et \quad (11)$$

$$k_{0,N}^{uniform} = \left(-0.07378\left(\frac{h}{b}\right)^4 + 2.38094\left(\frac{h}{b}\right)^3 - 9.91268\left(\frac{h}{b}\right)^2 + 32\left(\frac{h}{b}\right) - 28.71243\right)^{-1} \quad (12)$$

As is shown in Figure (7b), the reduction in the elastic stiffness of SSBDs with non-uniform ($k_{0,SSBD}^{non-uniform}$) compared with elastic stiffness of uniform SSBDs ($k_{0,SSBD}^{uniform}$) showed a linear correlation. A bilinear analytical expression is utilized to consider the effect of non-uniform edge shape on the elastic stiffness of SSBDs according to Equations (13) and (14).

$$X_{N.A} \le 0.25 \quad k_{0,SSDS}^{non-uniform} = k_{0,SSDS}^{uniform}(-3.501X_{N.A} + 1.036) \le k_{0,SSDS}^{uniform} \quad (13)$$

$$X_{N.A} > 0.25 \quad k_{0,SSDS}^{non-uniform} = k_{0,SSDS}^{uniform}(-0.9576X_{N.A} + 0.3865) \quad (14)$$
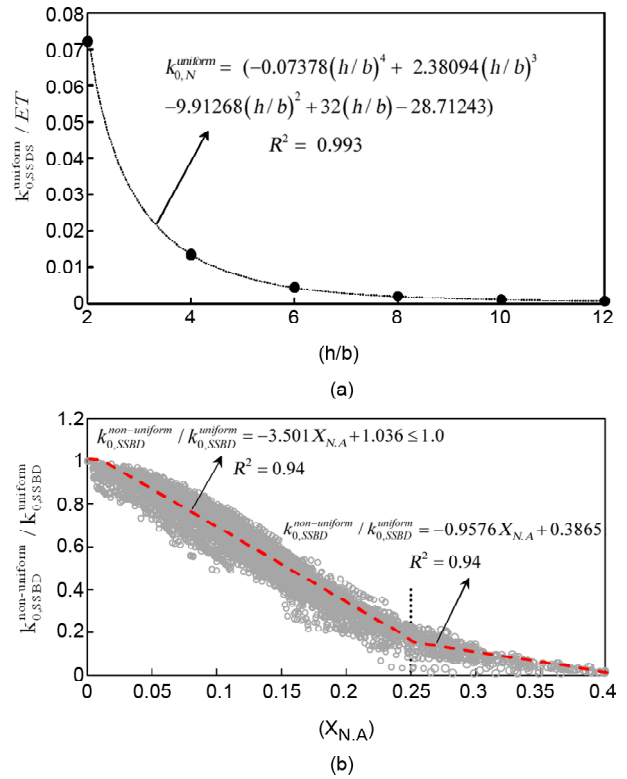
According to Figure (1a), considering the number

Figure 7. (a) Elastic Stiffness of single strip BDs with uniform side edges. (b) The ratio of elastic stiffness of non-uniform strips to those of uniform strips.

of strips equal to m, and the width and height of support plates equal to B and $(H-h)/2$, respectively, the elastic stiffness of an arbitrary BD can be considered as shear stiffness of two supporting plates in series with total stiffness of strips. Finally, the initial elastic stiffness of an arbitrary BD with two supporting plates at both ends (k_0^{BD}) can be expressed as follows:

$$k_0^{BD} = \frac{1}{\frac{1}{mk_{0,SSDS}^{non-uniform}} + \frac{\kappa(H-h)}{GBt}} \quad (15)$$

where G is the shear modulus of material and κ is the shape factor of a rectangular section for shear deformation and is equal to 1.2.

4.3. Hysteresis Response of Non-Uniform Models

Figure (8) shows the hysteresis responses for four uniform and corresponding non-models with different h/t and h/b ratios. The non-uniform models are selected among 10,000 random models created in the first group of FE models which showed the highest ductility and energy dissipation capacity
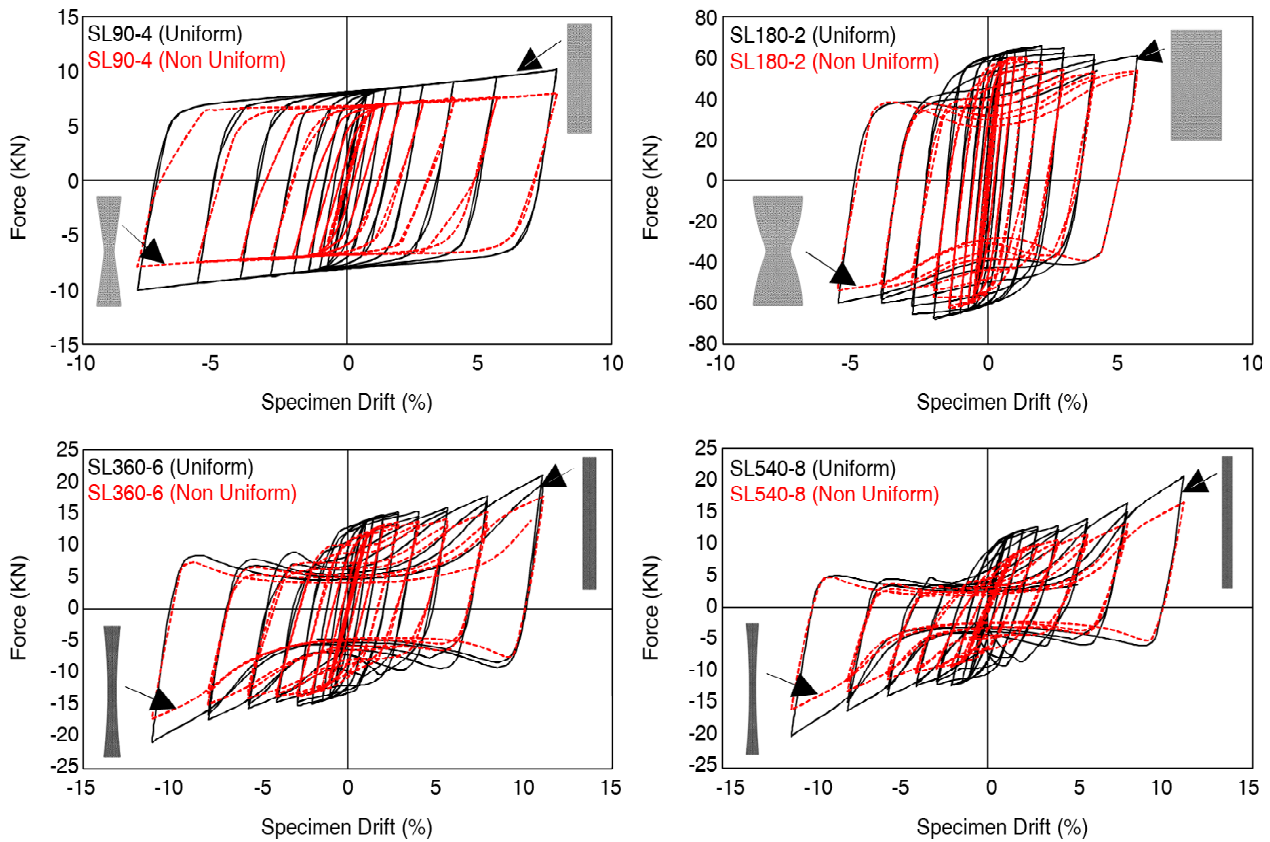
Figure 8. Cyclic response of uniform strip and corresponding butterfly strip [7].

among the random models.

As shown, the stiffness and ultimate strength of the non-uniform models decreased by removing plate material. A more severe pinching in the hysteresis curves of non-compact, non-uniform models is evident in comparison with those of uniform models as a result of premature buckling of non-uniform models. Although the pinching is commonly recognized as a factor in reducing the energy dissipation capacity of structural yielding components, in cases such as self-centering structures, the butterfly damper s with pinched hysteresis and high low-cycle-fatigue resistance could be functional to preserve the self-centering capability [7, 14, 18, 19].

4.4. The Behavioral Mechanism of Slender, Non-Uniform Strips

In the case of stocky BDs, the strips aspect ratio provides an appropriate measure for explaining the governing response of strips. In short compact strips (h/b <1.3), shear yielding of the plate is found to be predominant [20]. On the other hand, in long strips (h/b >5), the behavior of the damper is governed by flexural yielding [21]. However, for non-compact,

non-uniform BDs, the cyclic responses are not necessarily similar to the stocky dampers while significant pinched response observed in non-uniform strips as depicted in Figure (8).

The cyclic response and buckle shape of strips in B09-56 model, during the loading, are depicted in Figure (9). According to the observations, at the beginning of loading, prior to the occurrence of any buckling or yielding, the strips deformed in a double curvature (Figure 9a). The strips exhibited elastic flexural response upon the shear deformations with amplitudes less than 1.0 %. By increasing the deformation amplitudes, the first yielding of strips occurred at the one-quarter of the strip height from both ends (Figure 9b). By spreading the yielding to the entire height of strips (Figure 9c), the stiffness of strip suddenly dropped and consequently, severe buckling occurred (Figure 9d). From this phase onwards, as is evident in Figure (9-e), significant pinching in tension excitations and strength degradation in compression observed in the cyclic response of the model. By developing hinges with low stiffness and strength and occurrence of buckling, the axial response of the central portion of the strip with hinged ends governed the BDs response (Figure 9f).
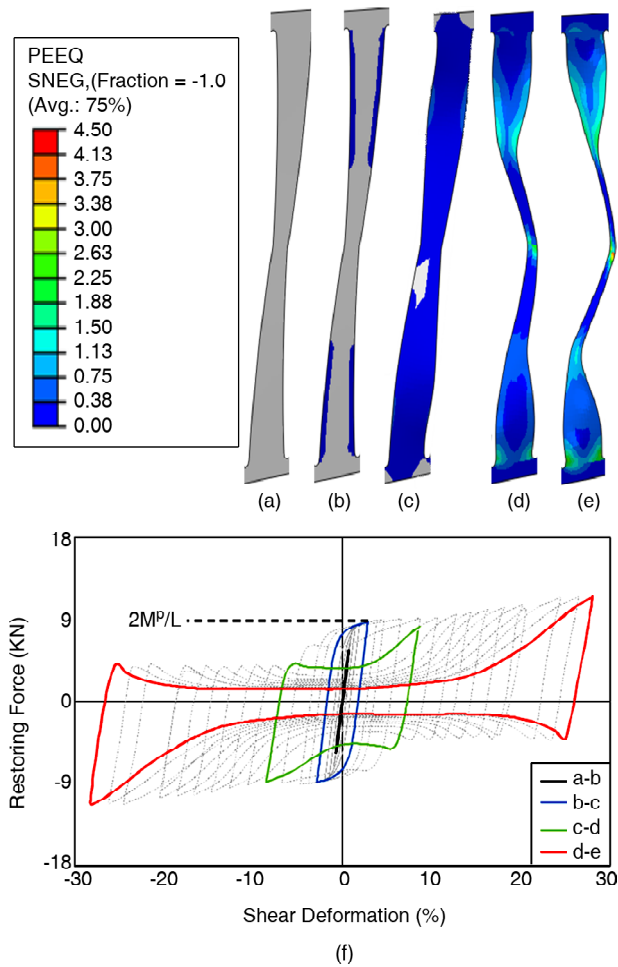
Figure 9. Cyclic behavioral mechanism strips in non-compact strips.

The minimum R-squared (R^2) value and average error between FEM results and the values obtained by the proposed equation were 0.9996 and 0.4% respectively. The buckling coefficient of non-uniform strips also exhibited a strong linear correlation with normalized average coordination of control points with respect to strip width ($X_{N.A}$).

❖ The elastic stiffness of single struts with fixed ends is correlated with aspect ratio and the shape of free, side edges. A quartic polynomial expression was proposed to predict the elastic stiffness of BDs with uniform strips, based on the FEM results. The R-squared and average errors were 0.993 and 1% respectively. Similar to the buckling coefficient of non-uniform strips, the elastic stiffness of strips with non-uniform shape compared with elastic stiffness of uniform strips showed a strong linear correlation.

❖ The ultimate response of non-compact, non-uniform strips, after the occurrence of buckling, was mainly governed by axial response of strips. Hence, the cyclic response of non-compact butterfly dampers is generally associated with a high pinching.

5. Conclusion

A finite element updating parametric study was carried out to evaluate the buckling, initial stiffness, and pinching response of non-uniform butterfly dampers. The accuracy of the FEM was verified and more than 10,000 random FE models developed during the finite element updating process. The buckling coefficient and initial stiffness of BDs with uniform and non-uniform side edges were proposed by a set of analytical expressions. The behavioral mechanism of strips was also discussed in detail. The main conclusions in the study are as follow:

❖ The buckling response of struts with fixed ends is highly dependent on the overall and cross-sectional aspect ratios as well as the relative area of removed parts. The buckling coefficient of BDs with uniform side edges was proposed with second-order polynomial relationships which take into account the influence of (t/b) and overall aspect ratio (b/h) of strips respectively.

References

1. Farzampour, A. and Eatherton, M. (2017) Lateral torsional buckling of butterfly-shaped shear links. *Proc. Annu. Stab. Conf. Struct. Stab. Res. Counc.*

2. Lee, C.H., Ju, Y.K., Min, J.K., Lho, S.H., and Kim, S.D. (2015) Non-uniform steel strip dampers subjected to cyclic loadings. *Engineering Structures*, **99**, 192-204.

3. Ghabraie, K., Chan, R., Huang, X., and Xie, Y.M. (2010) Shape optimization of metallic yielding devices for passive mitigation of seismic energy. *Engineering Structures*, **32**(8), 2258-2267.

4. Xian, M., Borchers, E., Pena, A., Krawinkler, H., Billington, S.L., and Deierlein, G.G. (2010) *Design and Behavior of Steel Shear Plates with Openings as Energy Dissipating Department of Civil and Environmental Engineering Design and Behavior of Steel Shear Plates with Openings as Energy Dissipating Fuses*. By Xiang Ma, Eric Borchers, Alex Pena, H. John A. Blume

Earthquake Engineering Center (Report No. 173).

5. Siar Mahmood Shah, A. and Moradi, S. (2020) Cyclic response sensitivity of energy dissipating steel plate fuses. *Structures*, **23**, 799-811.

6. Deng, K., Pan, P., Sun, J., Liu, J., and Xue, Y. (2014) Shape optimization design of steel shear panel dampers. *Journal of Constructional Steel Research*, **99**, 187-193.

7. Kiani, B.K., Hosseini, B., and Torabian, S. (2020) Optimization of slit dampers to improve energy dissipation capacity and low-cycle-fatigue performance. *Engineering Structures*, **214**, 110609.

8. Kiani, B.K, Torabian, S., and Mirghaderi, S.R. (2015) Local seismic stability of flanged cruciform sections (FCSs). *Engineering Structures*, **94**, 04.003.

9. Liu, Y. and Shimoda, M. (2013) Shape optimization of shear panel damper for improving the deformation ability under cyclic loading. *Structural and Multidisciplinary Optimization*, **48**(2), 427-435.

10. Zhang, C., Zhang, Z., and Shi, J. (2012) Development of high deformation capacity low yield strength steel shear panel damper. *Journal of Constructional Steel Research*, **75**, 116-130.

11. FEMA (2007) *Interim Protocols for Determining Seismic Performance Characteristics of Structural and Nonstructural Components*. Federal Emergency Management Agency, FEMA 461.

12. Farzampour, A. and Eatherton, M.R. (2019) Yielding and lateral torsional buckling limit states for butterfly-shaped shear links. *Engineering Structures*, **180**, 442-451.

13. Plaut, R.H. and Eatherton, M.R. (2017) Lateral-torsional buckling of butterfly-shaped beams with rectangular cross section. *Engineering Structures*, **136**, 210-218.

14. Ma, X., Borchers, E., Pena, A., Krawinkler, H., Billington, S., and Deierlein, G.G. (2010) *Design and Behavior of Steel Shear Plates with Openings as Energy-Dissipating Fuses*. Internal Report, John A. Blume Earthquake Engineering Center, Stanford University.

15. Hedayat, A.A. (2015) Prediction of the force displacement capacity boundary of an unbuckled steel slit damper. *Journal of Constructional Steel Research*, **114**, 30-50.

16. Trahair, N.S. (2003) *Guide to Stability Design Criteria for Metal Structures* (4th edition). John Wiley & Sons.

17. Alinia, M.M. and Dastfan, M. (2006) Behaviour of thin steel plate shear walls regarding frame members. *Journal of Constructional Steel Research*, **62**(7), 730-738.

18. Xian, M., Krawinkler, H., and Deierlein, G.G. (2010) *Seismic Design and Behavior of Self-Centering Braced Frame with Controlled Rocking and Energy-Dissipating Fuses*. John A. Blume Earthquake Engineering Center, 438.

19. Eatherton, M.R. and Hajjar, J.F. (2014) Hybrid simulation testing of a self-centering rocking steel braced frame system. *Earthquake Engineering and Structural Dynamics*, **43**(11), 1725-1742.

20. Oh, S.H., Kim, Y.J., and Ryu, H.S. (2009) Seismic performance of steel structures with slit dampers. *Engineering Structures*, **31**(9), 1997-2008.

21. Lee, J. and Kim, J. (2017) Development of box-shaped steel slit dampers for seismic retrofit of building structures. *Engineering Structures*, **150**, 934-946.